Human Molecular Genetics, 1995, Vol. 4, No. 11 2145–2150

A duplication/paracentric inversion associated with familial X-linked deafness (DFN3) suggests the presence of a regulatory element more than 400 kb upstream of the *POU3F4* gene

Yvette J.M.de Kok*, Gerard F.M.Merkx, Silvère M.van der Maarel, Irene Huber, Susan Malcolm[1], Hans-Hilger Ropers and Frans P.M.Cremers

Department of Human Genetics, University Hospital Nijmegen, Geert Grooteplein Zuid 20, 6525 GA Nijmegen, The Netherlands and [1]Institute of Child Health, University of London, 30 Guilford Street, London WC1N 1EH, UK

Received July 10, 1995; Revised and Accepted August 24, 1995

X-linked deafness with stapes fixation (DFN3) is caused by mutations in the *POU3F4* gene at Xq21.1. By employing pulsed field gel electrophoresis (PFGE) we identified a chromosomal aberration in the DNA of a DFN3 patient who did not show alterations in the open reading frame (ORF) of *POU3F4*. Southern blot analysis indicated that a DNA segment of 150 kb, located 170 kb proximal to the *POU3F4* gene, was duplicated. Fluorescence *in situ* hybridization (FISH) analysis, PFGE, and detailed Southern analysis revealed that this duplication is part of a more complex rearrangement including a paracentric inversion involving the Xq21.1 region, and presumably the Xq21.3 region. Since at least two DFN3-associated minideletions are situated proximal to the duplicated segment, the inversion most likely disconnects the *POU3F4* gene from a regulatory element which is located at a distance of at least 400 kb upstream of the *POU3F4* gene.

INTRODUCTION

The most frequent form of X-linked deafness, DFN3, is characterized by fixation of the stapes and a perilymphatic gusher upon stapedectomy. By employing computerized tomography, Phelps *et al.* (1) identified a unique abnormality of the petrous temporal bone consisting of a dilatation of the internal auditory meatus (IAM) and an abnormal wide communication between the basal turn of the cochlea and the IAM. The gene underlying DFN3 was mapped to Xq21 by linkage analysis and through molecular characterization of large deletions associated with choroideremia, mental retardation, and DFN3 (2–7). Smaller deletions were found in five patients with typical DFN3 (8–11). Yeast artificial chromosome (YAC) clones that span the critical region were isolated, and an 850 kb cosmid contig was constructed (9).

Recently, Douville *et al.* (12) assigned a mouse POU domain gene, *Brain 4*, to a region of the murine X chromosome that is homologous to human Xq13–q22. The rat homolog of *Brain 4*, *RHS2*, is expressed during embryonic development in the brain, the neural tube, the whisker roots, and the otic vesicle (13). We cloned and characterized the human homolog of *Brain 4*, *POU3F4*, and were able to position the gene in the critical region for DFN3. In seven unrelated patients with DFN3 but not in 100 control X-chromosomes, small mutations were found in the *POU3F4* gene that result in truncation of the predicted protein or in non-conservative amino acid substitutions (14,15). Surprisingly, the intronless *POU3F4* gene was found to be located up to 400 kb distal to four minideletions associated with typical DFN3 (11,14).

Here, we describe the identification and detailed characterization of another, more complex chromosomal rearrangement, a duplication/paracentric inversion associated with familial DFN3. We show that one of the inversion breakpoints is situated 320 kb proximal to *POU3F4*. Since at least two DFN3 associated minideletions reside proximal to the duplication, this finding suggests that the expression of *POU3F4* is regulated by a sequence element located several hundred kilobases farther proximal.

RESULTS

Identification of a duplication associated with DFN3 by PFGE and Southern blot analysis

We performed pulsed field gel electrophoresis analysis of genomic DNA of several DFN3 patients using a cosmid (4893F6; Fig. 5) located in the Xq21.1 region proximal to the *POU3F4* gene. In the DNA of DFN3 patient 5086, we observed a *Sfi*I fragment of 575 kb instead of the normal 675 kb, suggestive of a microdeletion or a *Sfi*I restriction fragment length polymorphism (Fig. 1a). Southern blot analysis of *Eco*RI digested DNA of patient 5086 employing all cosmids from a previously established 850 kb contig did not yield a deletion. In contrast, the hybridization signals of several cosmids near the DXS26 locus suggested the presence of a duplicated DNA fragment (data not shown). To investigate this possibility in more detail, we constructed *Eco*RI and *Taq*I blots containing equal amounts of DNA from a control female, a control male, DFN3 patient 5086, and patient XL45. The latter patient carries a microscopically visible deletion com-

*To whom correspondence should be addressed

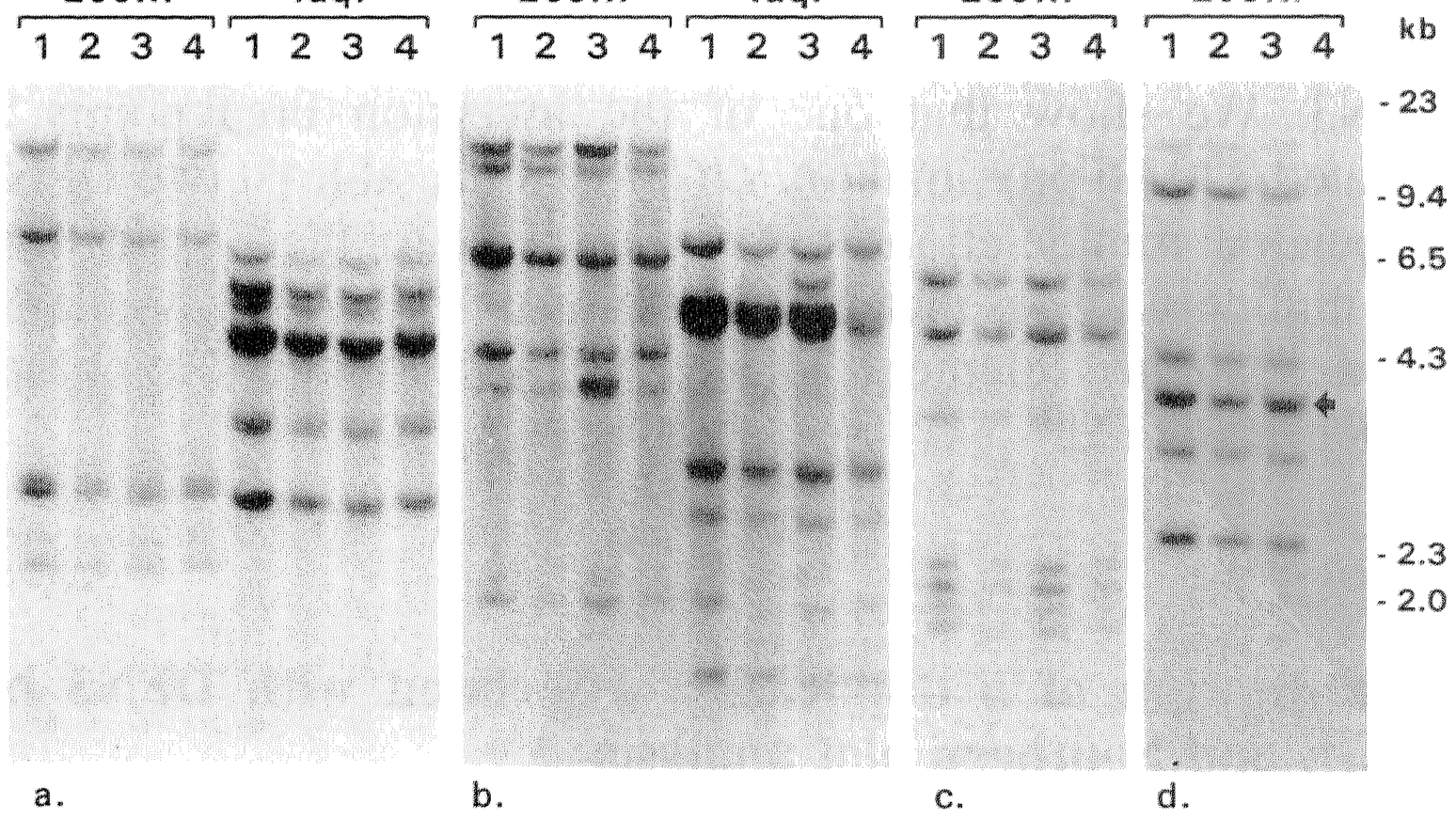

Figure 2. Southern blot analysis of genomic DNAs from a control female (lane 1), control male (lane 2), DFN3 patient 5086 (lane 3), and the syndromic DFN3 patient XL45 (lane 4). The restriction enzymes and hybridization probes used are indicated on top of each panel. **(a)** Cosmid 4893D9 detects restriction fragments of equal intensity in patient 5086 and the control male. **(b)** Cosmid 4893A1 detects signals of normal and double intensity as well as aberrantly sized *Eco*RI (4.0 kb) and *Taq*I (6.0 kb) fragments in patient 5086. **(c)** Cosmid 4893B4 detects signals with a double intensity in patient 5086 compared to a male control. **(d)** Cosmid 4893C4 detects one fragment (indicated with an arrow) which is either of double intensity compared to the male control lane, or represents a novel aberrantly sized fragment. Size markers are given on the right.

mencing in the region investigated here. In patient 5086, a double intensity of *Eco*RI and *Taq*I bands compared to control male DNA was observed for cosmids 4893B4 (Fig. 2c), 4893K6, 4893B5, 4893K2, and 4893H12 (Fig. 5; Southern

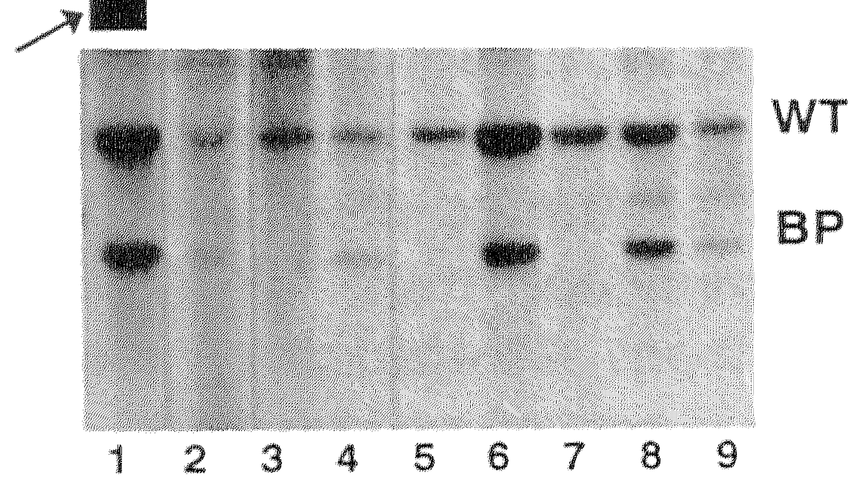

Figure 4. Southern blot analysis of *Eco*RI digested DNA from patient 5086 (arrow) and several of his relatives. The 6.5 kb *Eco*RI fragment of cosmid 4893A1 was employed as a probe. WT = wildtype; BP = breakpoint.

blot data not shown). Cosmid 4893A1 detects restriction fragments with a normal intensity, a double intensity, as well as an aberrantly sized *Eco*RI (4.0 kb) and *Taq*I (6.0 kb) fragment (Fig. 2b). All cosmids proximal to 4893A1 showed normal hybridization results, as illustrated by cosmid 4893D9 (Fig. 2a). For cosmid 4893C4, only a 4.0 kb *Eco*RI band appeared to be of double intensity compared to control male DNA (Fig. 2d); no aberrantly sized fragments were detected. All cosmids distal to 4893C4 showed normal hybridization results (data not shown).

Detailed mapping of the duplication endfragments and family analysis

The endfragments of the duplicated segment in patient 5086 were mapped in detail by analysing genomic DNA from patient 5086 and an unaffected control individual with *Eco*RI fragments from cosmids 4893A1 and 4893C4. At the proximal end, a 6.5 kb *Eco*RI fragment of cosmid 4893A1 detected 4.0

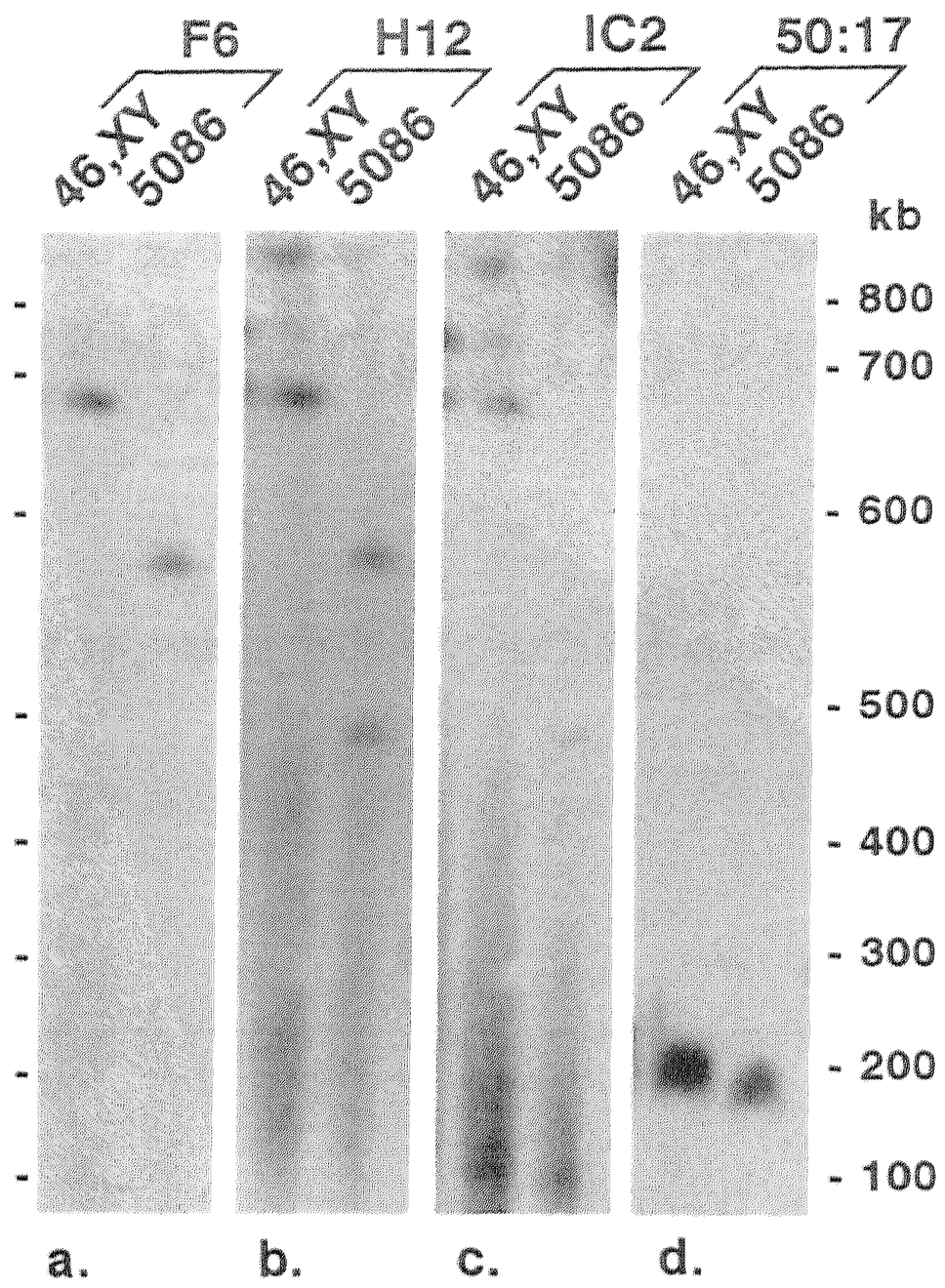

Figure 1. PFGE analysis of *Sfi*I digested high-molecular-weight DNA from a male control and DFN3 patient 5086. Hybridization results are shown for cosmid 4893F6 (**a**), cosmid 4893H12 (**b**), cosmid IC2 (**c**) and for a control probe 50:17 (**d**), located in Xq13.1 (van der Maarel *et al.* manuscript in preparation). The scale shown on the right is based on the migration of the *Saccharomyces cerevisiae* chromosomes which were employed as size markers.

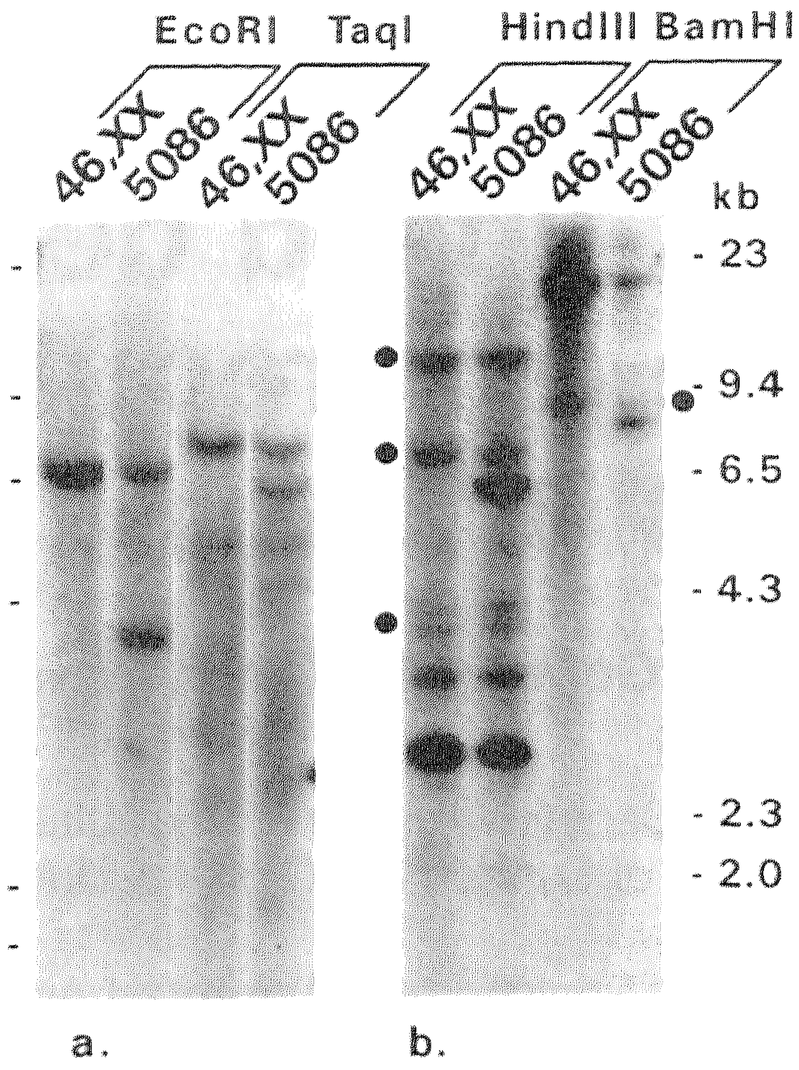

Figure 3. Molecular characterization of the duplication/inversion endpoints in patient 5086. Southern blot analysis of genomic DNAs digested with the enzymes given above the lanes using a 6.5 kb *Eco*RI fragment of cosmid 4893A1 (**a**) and a 1.7 kb *Eco*RI fragment of cosmid 4893C4 (**b**). Black dots mark the signals from a previous hybridization. Size markers are given on the right.

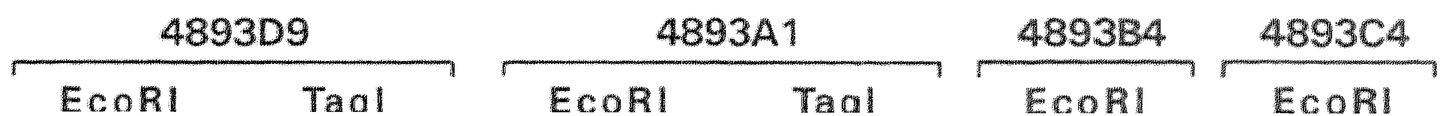

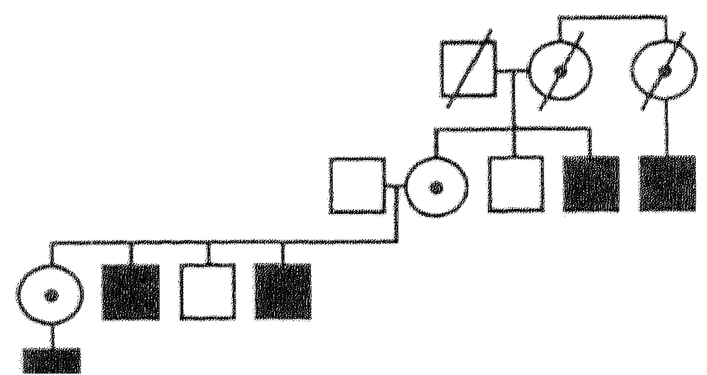

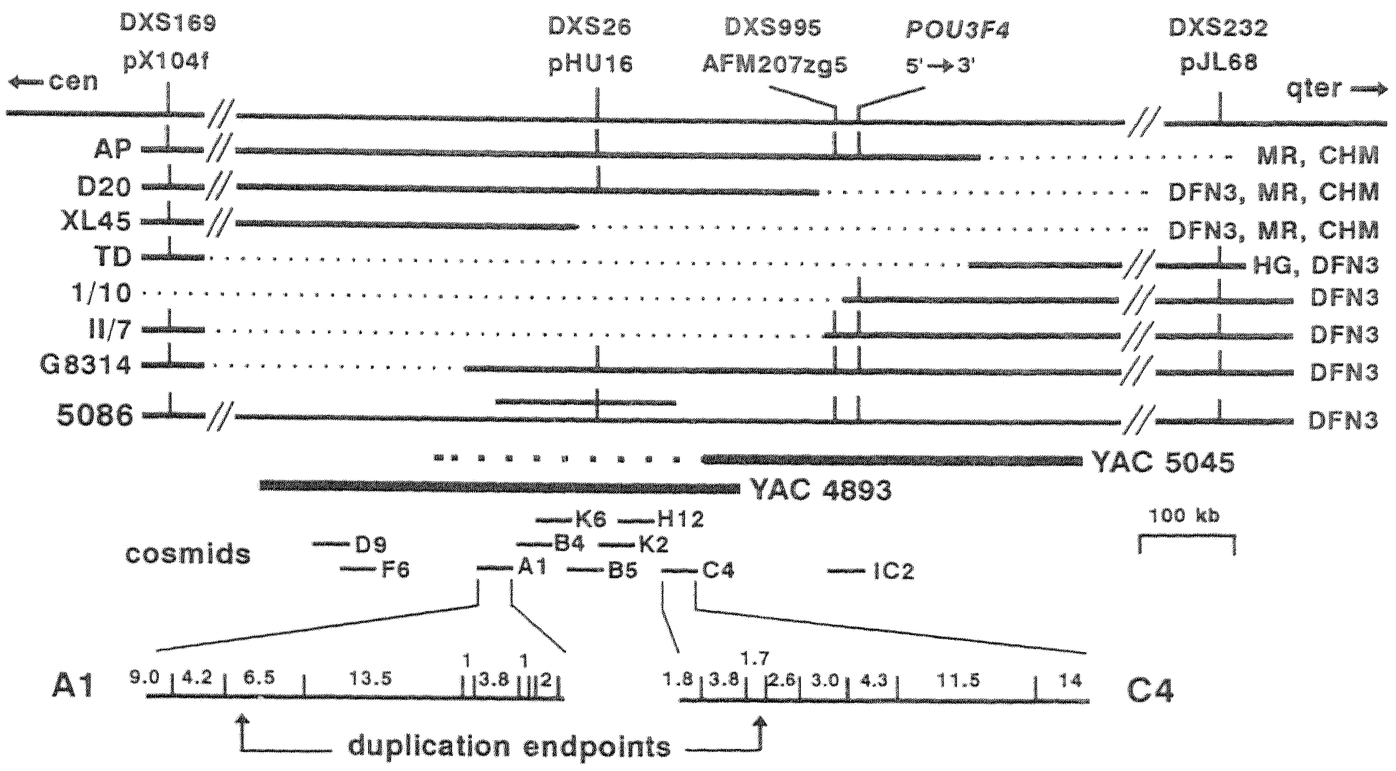

Figure 5. Physical map of the DFN3 critical region. All patients with deletions except AP have been described elsewhere (9,20). Patient AP shows choroideremia (CHM) and mental retardation (MR) (20). Deletions are indicated by stippled lines. The duplicated segment in patient 5086 is depicted by a double bar. *Eco*RI maps of the cosmids spanning the duplication breakpoints are given at the bottom. *Eco*RI fragment sizes are given in kilobases. Only a subset of the cosmids from the contig is depicted. DFN3 = X-linked deafness with stapes fixation; HG = hypogonadism.

kb *Eco*RI and 6.0 kb *Taq*I breakpoint fragments (Fig. 3a). Since we were unable to identify aberrantly sized fragments with cosmid 4893C4 in *Eco*RI and *Taq*I digested DNA of patient 5086, blots were constructed containing *Hin*dIII and *Bam*HI digested DNAs. The distal endpoint of the duplication could be detected with a 1.7 kb *Eco*RI fragment from cosmid 4893C4 which, in addition to normally sized restriction fragments, clearly hybridizes to novel *Hin*dIII and *Bam*HI fragments (Fig. 3b). Based on the signal intensities observed, the distal duplication breakpoint is located in a 2.8 kb *Hin*dIII and a 18 kb *Bam*HI fragment. From the previously established *Eco*RI restriction map of the cosmid contig, we estimate that the duplicated DNA segment measures 150 kb (Fig. 5).

To investigate whether this rearrangement segregates with the DFN3 phenotype in the family of patient 5086, we hybridized the 6.5 kb *Eco*RI fragment of cosmid 4893A1 to a Southern blot containing *Eco*RI digested DNAs from several family members. Clearly, the breakpoint fragment indicative of the chromosomal rearrangement can be seen in all DFN3 patients and female carriers (Fig. 4).

FISH and PFGE analysis

To investigate whether the two copies of the duplicated segment are located next to each other near the *POU3F4* gene, a cosmid located on the duplicated segment, 4893H12, was hybridized to metaphase chromosomes prepared from an EBV-immortalized lymphoblastoid cell line of patient 5086. In most chromosome spreads, the X-chromosome showed two specific, but rather diffuse signals (Fig. 6a). To our surprise, we observed four discrete signals in approximately one-third of the metaphases investigated, indicating that cosmid 4893H12 hybridizes to two different regions of the X-chromosome of patient 5086 (Fig. 6b,c). In a control metaphase X-chromosome, 4893H12 identified one distinct locus in the Xq21 band (data not shown). The most straightforward explanation for the FISH and Southern blotting results is a duplication-paracentric inversion event which moved one of the copies of the duplicated segment away from the endogenous copy of cosmid 4893H12 (Fig. 7).

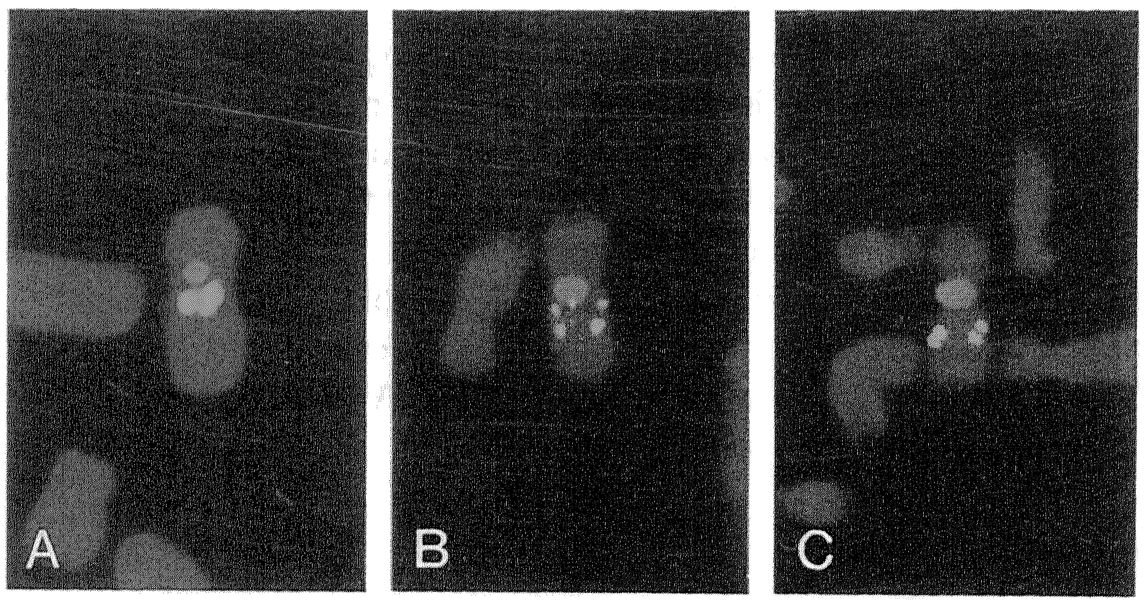

Figure 6. FISH analysis of three X-chromosomes in a metaphase chromosome spread of EBV-immortalized peripheral blood cells of patient 5086 using the centromere X probe (pBAMX5), detected in red, in conjunction with probe 4893H12, detected in yellow/green. Chromosomes are counterstained using the blue dye DAPI.

To test this hypothesis, cosmid 4893H12 and cosmid IC2, the latter of which contains the *POU3F4* gene, were successively employed as probes on the PFGE blot described above. As expected, cosmid 4893H12 detected the 575 kb *Sfi*I fragment identified by cosmid 4893F6, corresponding to one of the inversion breakpoints, and an additional 475 kb *Sfi*I fragment (Fig. 1b). Since the latter fragment is also identified by cosmid IC2 (Fig. 1c), it most likely spans the other inversion-breakpoint as indicated in Figure 7. To investigate whether the inversion involves chromosomal sequences proximal or distal to the *POU3F4* gene, FISH analysis was performed with differently labeled cosmids from the duplication (4893H12) and the choroideremia (*CHM*) gene (cosmid U98B5) located at Xq21.2. In only one X-chromosome, the *CHM* cosmid could be localized between the duplicated sequences; in all other metaphase chromosome spreads analysed, the 4893H12 and U98B5 signals were not resolved (data not shown).

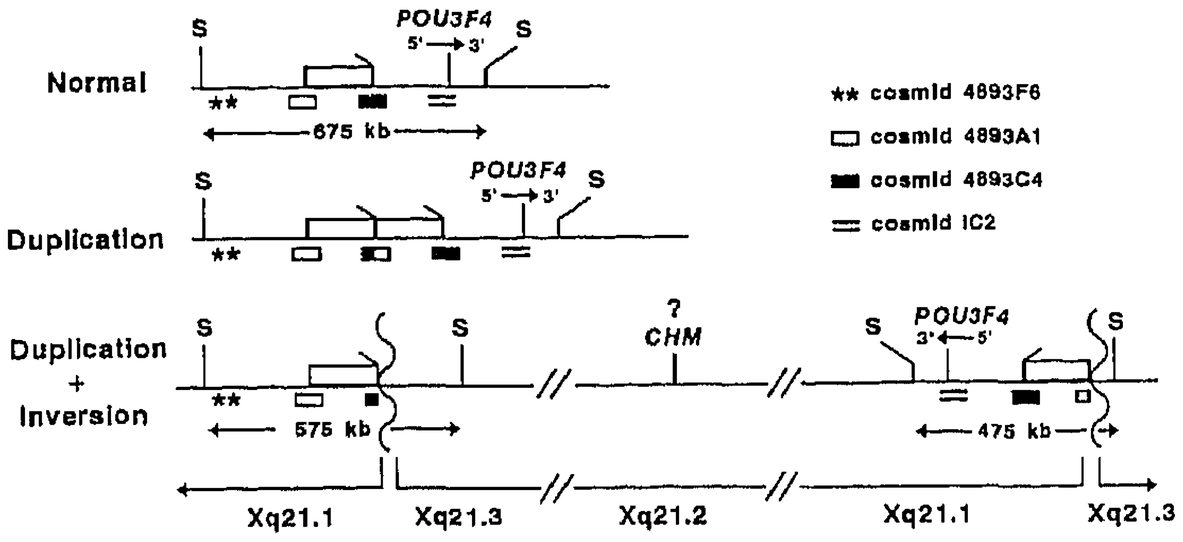

Figure 7. Model for the duplication/paracentric inversion event that gave rise to the observed rearrangement in DFN3 patient 5086. The upper drawing reflects the normal situation; the middle shows an intermediate structure resulting from a DNA duplication event; the lower schematic illustrates the proposed final rearrangement observed in patient 5086. The locations of the *Sfi*I (S) sites flanking the duplicated segment were derived from the cosmid contig (unpublished data). The locations of the *Sfi*I sites in the Xq21.3 region were deduced from the observed *Sfi*I fragment sizes (see Fig. 1).

POU3F4 analysis in patient 5086

DNA of patient 5086 was examined for single strand conformation (SSC) variants by employing PCR primer sets defining five overlapping DNA segments that span the entire coding sequence of the *POU3F4* gene (14). All five DNA segments could be readily amplified indicating no apparent structural abnormality in the protein coding region of *POU3F4*. No SSC shifts indicative of sequence alterations were found. The entire ORF of *POU3F4* was analysed by DNA sequencing but no abnormalities were found.

DISCUSSION

We have identified and characterized a complex rearrangement in a patient with DFN3. The results of PFGE and Southern blot analysis are not consistent with a simple tandem duplication event, i.e. insertion of the new copy adjacent to the endogenous sequence proximal to the *POU3F4* gene. Since *Sfi*I restriction sites are known to flank the duplicated segment (Fig. 7), this event would generate a 825 kb *Sfi*I band and not the observed 575 kb *Sfi*I band. FISH analysis using a cosmid from the duplicated segment showed that the duplicated segments are separated by several megabases of DNA. Results of PFGE and Southern blotting are compatible with a duplication/paracentric inversion involving sequences at Xq21.1 near *POU3F4*, and Xq13.3 or Xq21.3. In agreement with this, cosmid 4893H12, located on the duplicated segment, and cosmid IC2, spanning the *POU3F4* gene, detected an additional *Sfi*I fragment corresponding to the other breakpoint of the inversion (Fig. 1b,c). FISH analysis suggests that the *CHM* gene at Xq21.2 is located between the duplicated segments. Also, positioning of the duplicated segments along the X-chromosome suggests locations at Xq21.1 and Xq21.3, although the involvement of the Xq13 band cannot be ruled out completely. Both high resolution metaphase FISH analysis as well as detailed PFGE analysis using cosmids distal to the *CHM* gene will enable the precise positioning of this breakpoint.

The duplication/inversion event proposed here does not affect the *POU3F4* gene proper, which, in the rearranged situation (Fig. 7), is situated 170 kb proximal to one copy of the duplicated segment and 320 kb proximal to the distal inversion breakpoint. To explain the DFN3 phenotype in patient 5086, as well as the aforementioned minideletions situated proximal to the *POU3F4* gene, a few possibilities are considered. First, in the normal situation, the 5′ part of the *POU3F4* gene, including its promoter, might be situated farther centromeric. In this situation, the *POU3F4* gene would contain a single, unusually large intron (>400 kb) in its 5′ untranslated region (Fig. 5). We have located the 3′ end of the *POU3F4* mRNA 2.4 kb downstream of the ORF. Since the *POU3F4* mRNA was estimated to be 3.5 kb in size, we can deduce that the 5′ untranslated region measures less than 200 bp (unpublished data). From these findings we deduce that most probably, there is no large 5′ intron in the *POU3F4* gene. Second, another gene involved in DFN3 might be situated in the chromosomal segment proximal to *POU3F4*. If so, this gene would be predicted to span a region of more than 200 kb, the distance between the proximal inversion-breakpoint observed in patient 5086 and the DFN3 associated deletion mapping farthest centromeric (G8314; Fig. 5). We believe that this is an unlikely possibility, too, since this chromosomal segment was found to be devoid of sequences transcribed in fetal brain tissue. In a third model, the three minideletions and the duplication/inversion would juxtapose heterochromatic sequences from Xq21.1 and Xq21.3 respectively, near the *POU3F4* gene, which then might down-regulate transcription of the *POU3F4* gene. In *D.melanogaster*, translocation of genes into heterochromatin is known to give rise to cell-autonomous gene silencing, a phenomenon called position effect variegation (16). In humans, examples of position effects are rare. Campomelic dysplasia, a skeletal malformation syndrome and autosomal sex reversal, is not only caused by mutations in the *SOX9* gene, but also by translocations involving sequences located more than 50 kb away from the *SOX9* gene (17,18). Similarly, translocations up to 85 kb from the *PAX6* gene are causally related to the aniridia phenotype (19). If this mechanism plays a role in the Xq21 region, it is directional in nature, since a large deletion 120 kb distal to the *POU3F4* gene (patient AP; Fig. 4), is associated with mental retardation and choroideremia, but not with hearing impairment (20). It remains to be investigated whether transcriptional silencing of the respective genes is due to position effects.

To explain the DFN3 phenotype in patient 5086, we favour a model in which the proposed inversion separates a control element, most likely an enhancer element, from the *POU3F4* transcription unit. A similar situation was reported for the α- and β-globin gene clusters in which deletions remove important control regions (21,22). To account for the clinical findings in all patients with minideletions [patients I/10, II/7, G8314 (Fig. 4) and patient ML (11)] that do not span the *POU3F4* gene, the putative enhancer sequence should be located more than 400 kb upstream of the gene. Since in none of these patients mutations were found in the ORF of the *POU3F4* gene (14; Y.J.M.de K. and F.P.M.C., unpublished data), the deletions must be causative for the observed phenotype. It is noteworthy that the deletion in patient II/7 is accompanied by a paracentric inversion. The breakpoints in

this familial case are in Xq13.1 and Xq21.2 (23). Thus far, we were unable to test our hypothesis directly since reverse transcription-PCR analysis of the *POU3F4* mRNA isolated from control lymphoblast failed, indicating that POU3F4 expression in lymphoblasts is very low.

In three patients with DFN3 we were unable to find causative mutations in or outside the DFN3 gene. If the expression of this gene depends on the presence of an enhancer situated proximal to the *POU3F4* gene, small mutations or chromosomal abnormalities might be found in the chromosomal region centromeric to the cosmid contig. To investigate this region in more detail, a YAC clone from this particular region was recently isolated (20) and the construction of a cosmid contig is underway. Elucidation of the molecular mechanism responsible for the DFN3 phenotype in patients with structural abnormalities at a large distance from the *POU3F4* gene will yield important new insights into the regulation of this gene.

MATERIALS AND METHODS

DFN3 patients

Patient 5086 is the youngest member of a multigeneration deafness family (24; Fig. 4). Audiologic examination showed a profound sensorineural hearing loss. Two maternal uncles of the proband showed a total hearing loss. Radiological examination using computerized tomography in patient 5086 and two maternal uncles revealed dilated internal auditory canals and structural lesions of the cochlea that cause an incomplete separation of perilymphatic and cerebrospinal fluids. The mother of the proband showed a moderate mixed hearing loss in a pure tone audiogram (24). Together, these findings suggest that the deafness in this family can be classified as DFN3. In most patients with DFN3, both sensorineural and conductive hearing loss is found. In this case the conductive element is probably masked by the profound sensorineural component. Patient XL45 suffers from DFN3, mental retardation and choroideremia, and has been described in more detail elsewhere (7,25,26).

Pulsed field gel electrophoresis and Southern blotting

PFGE and Southern blot analysis were performed as described by Bach *et al.* (7) and Huber *et al.* (9), respectively. Cosmid IC2 corresponds to the ICRF clone c104L0131. Clone 50:17 (DXS6673E) is a cDNA constituting part of a gene spanning an Xq13.1 translocation breakpoint which is possibly involved in mental retardation (Van der Maarel *et al.*, in preparation).

Single strand conformation analysis and nucleotide sequencing

Polymerase chain reaction-single strand conformation (PCR-SSC) analysis (27) was performed employing five partially overlapping PCR segments spanning the ORF of *POU3F4* as described elsewhere (14).

Fluorescence *in situ* hybridization

All fluorescence *in situ* hybridization (FISH) procedures used were essentially as described previously (28–30). Briefly, cosmid 4893H12 was labeled with dig-11-dUTP (Boehringer) and the X centromere probe pBAMX5 with Fluorolink Cy3-dCTP (BDS inc. Pittsburgh) using a nick-translation kit (Gibco, Life Technologies). 100 ng labeled 4893H12 probe DNA and 5 μg Cot-1 DNA (Gibco, Life Technologies) was dissolved in 6 μl of a hybridization solution (50% v/v deionized formamide, 10% w/v dextrane sulphate, 2×SSC, 1% v/v Tween-20, pH 7.0). Prior to hybridization, the probe was denatured at 80°C for 10 min, chilled on ice, and incubated at 37°C for 30 min allowing preannealing. For pBAMX5 20 ng DNA in 6 μl was used per reaction and no competitor DNA was added. Metaphase spreads were prepared using standard procedures. After denaturation of the slides, probe incubations were carried out under an 18×18 mm coverslip in a moist chamber for 45 h.

Immunocytochemical detection of the hybridizing probes was achieved using FITC conjugated sheep-anti-digoxigenin (1:20, Boehringer Mannheim). For evaluation of the chromosomal slides a Zeiss epifluorescence microscope equipped with appropriate filters for visualization of Texas Red, DAPI and FITC fluorescence was used. Digital images were acquired using a high-performance cooled CCD camera (Photometrics, Tucson, USA), interfaced to a Macintosh IIci computer. All digital image-acquiring, -processing and -analysis functions were accomplished by means of the BDS-Image™ FISH software package (Biological Detection Systems Inc., Rockville, USA).

ACKNOWLEDGEMENTS

The authors thank S.D.van der Velde-Visser and E.Boender-van Rossum for technical assistance in cell culturing. We thank Drs M.Bitner-Glindzicz and M.E.Pembrey for helpful suggestions. The research of F.P.M.C. has been made possible by a fellowship of the Royal Netherlands Academy of Arts and Sciences. Y.J.M.de K. and I.H. were supported by the Netherlands Organization for Scientific Research (NWO).

REFERENCES

1. Phelps, P.D., Reardon, W., Pembrey, M., Bellman, S. and Luxon, L. (1991) X-linked deafness, stapes gushers and a distinctive defect of the inner ear. *Neuroradiology*, **33**, 326–330.
2. Rosenberg, T., Schwartz, M., Niebuhr, E., Yang, H.-M., Sardemann, H., Andersen, O. and Lundsteen, C. (1986) Choroideremia in interstitial deletion of the X chromosome. *Ophthalmic. Paediatr. Genet.*, **7**, 205–210.
3. Cremers, F.P.M., van de Pol, T.J.R., Wieringa, B., Hofker, M.H., Pearson, P.L., Pfeiffer, R.A., Mikkelsen, M., Tabor, A. and Ropers, H-H. (1988) Molecular analysis of male-viable deletions and duplications allows ordering of 52 DNA probes on proximal Xq. *Am. J. Hum. Genet.*, **43**, 452–461.
4. Cremers, F.P.M., van de Pol, T.J.R., Diergaarde, P.J., Wieringa, B., Nussbaum, R.L., Schwartz, M. and Ropers, H-H. (1989) Physical fine mapping of the choroideremia locus using Xq21 deletions associated with complex syndromes. *Genomics*, **4**, 41–46.
5. Cremers, F.P.M., Sankila, E.-M., Brunsmann, F., Jay, M., Jay, B., Wright, A., Pinckers, A.J.L.G., Schwartz, M., van de Pol, T.J.R., Wieringa, B., de la Chapelle, A., Pawlowitzki, I.H. and Ropers, H-H. (1990) Deletions in patients with classical choroideremia vary in size from 45 kb to several megabases. *Am. J. Hum. Genet.*, **47**, 622–628.
6. Merry, D.E., Lesko, J.G., Sosnoski, D.M., Lewis, R.A., Lubinsky, M., Trask, B., van den Engh, G., Collins, F.S. and Nussbaum, R.L. (1989) Choroideremia and deafness with stapes fixation: A contiguous gene deletion syndrome in Xq21. *Am. J. Hum. Genet.*, **45**, 530–540.
7. Bach, I., Robinson, D., Thomas, N., Ropers, H.-H. and Cremers, F.P.M. (1992) Physical fine mapping of genes underlying X-linked deafness and non fra(X)-X-linked mental retardation at Xq21. *Hum. Genet.*, **89**, 620–624.
8. Bach, I., Brunner, H.G., Beighton, P., Ruvalcaba, R.H.A., Reardon, W., Pembrey, M.E., van der Velde-Visser, S.D., Bruns, G.A.P., Cremers, C.W.R.J., Cremers, F.P.M. and Ropers, H-H. (1992) Microdeletions in patients with gusher-associated, X-linked mixed deafness (DFN3). *Am. J. Hum. Genet.*, 50, 38–44.
9. Huber, I., Bitner-Glindzicz, M., de Kok, Y.J.M., van der Maarel, S.M., Ishikawa-Brush, Y., Monaco, A.P., Robinson, D., Malcolm, S., Pembrey, M.E., Brunner, H.G., Cremers, F.P.M. and Ropers, H.-H. (1994) X-linked mixed deafness (DFN3): cloning and characterization of the critical region allows the identification of novel microdeletions. *Hum. Mol. Genet.*, **3**, 1151–1154.
10. Piussan, C., Hanauer, A., Dahl, N., Mathieu, M., Kolski, C., Biancalana, V., Heyberger, S. and Strunski, V. (1995) X-linked progressive mixed deafness: a new microdeletion that involves a more proximal region in Xq21. *Am. J. Hum. Genet.*, **56**, 224–230.
11. Dahl, N., Laporte, J., Hu, L., Biancalana, V., Le Paslier, D., Cohen, D., Piussan, C. and Mandel, J.L. (1995) Deletion mapping of X-linked mixed deafness (DFN3) identifies a 265–525-kb region centromeric of DXS26. *Am. J. Hum. Genet.*, **56**, 999–1002.
12. Douville, P.J., Atanasoski, S., Tobler, A., Fontana, A. and Schwab, M.E. (1994) The brain-specific POU-box gene *Brn4* is a sex-linked transcription factor located on the human and mouse X chromosomes. *Mamm. Genome*, **5**, 180–182.
13. le Moine, C. and Young, W.S., III (1992) *RHS2*, a POU domain-containing gene, and its expression in developing and adult rat. *Proc. Natl Acad. Sci. USA*, **89**, 3285–3289.
14. de Kok, Y.J.M., van der Maarel, S.M., Bitner-Glindzicz, M., Huber, I., Monaco, A.P., Malcolm, S., Pembrey, M.E., Ropers, H.-H. and Cremers, F.P.M. (1995) Association between X-linked mixed deafness and mutations in the POU domain gene *POU3F4*. *Science*, **267**, 685–688.
15. Bitner-Glindzicz, M., Turnpenny, P., Höglund, P., Kääriäinen, H., Sankila, E.-M., van der Maarel, S.M., de Kok, Y.J.M., Ropers, H.-H., Cremers, F.P.M., Pembrey, M. and Malcolm, S. (1995) Further mutations in *Brain 4* (POU3F4) clarify the phenotype in the X-linked deafness, DFN3. *Hum. Mol. Genet.*, **4**, 1467–1469.

16. Henikoff, S. (1990) Position-effect variegation after 60 years. *Trends Genet.*, **6**, 422–426.
17. Foster, J.W., Dominguez-Steglich, M.A., Guioli, S., Kwok, C., Weller, P.A., Stevanovic, M., Weissenbach, J., Mansour, S., Young, I.D., Goodfellow, P.N., Brook, J.D. and Schafer, A.J. (1994) Campomelic dysplasia and autosomal sex reversal caused by mutations in an *SRY*-related gene. *Nature*, **372**, 525–530.
18. Wagner, T., Wirth, J., Meyer, J., Zabel, B., Held, M., Zimmer, J., Pasantes, J., Dagna Bricarelli, F., Keutel, J., Hustert, E., Wolf, U., Tommerup, N., Schempp, W. and Scherer, G. (1994) Autosomal sex reversal and campomelic dysplasia are caused by mutations in and around the *SRY*-related gene *SOX9*. *Cell*, **79**, 1111–1120.
19. Fantes, J., Redeker, B., Breen, M., Boyle, S., Brown, J., Fletcher, J., Jones, S., Bickmore, W., Fukushima, Y., Mannens, M., Danes, S., van Heyningen, V. and Hanson, I. (1995) Aniridia-associated cytogenetic rearrangements suggest that a position effect may cause the mutant phenotype. *Hum. Mol. Genet.*, **4**, 415–422.
20. van der Maarel, S.M., Scholten, I.H.J.M., Maat-Kievit, J.A., Huber, I., de Kok, Y.J.M., de Wijs, I., van de Pol, T.J.R., van Bokhoven, H., den Dunnen, J.T., van Ommen, G.J.B., Philippe, C., Monaco, A.P., Smeets, H.J.M., Ropers, H.-H. and Cremers, F.P.M. (1995) Yeast artificial chromosome cloning of the Xq13.3–q21.31 region and fine mapping of a deletion associated with choroideremia and non-specific mental retardation. *Eur. J. Hum. Genet.*, in press.
21. Grosveld, F., Blom van Assendelft, G., Greaves, D.R. and Kollias, G. (1987) Position-independent, high-level expression of the human β-globin gene in transgenic mice. *Cell*, **51**, 975–985.
22. Higgs, D.R., Wood, W.G., Jarman, A.P., Sharpe, J., Lida, J., Pretorius, I.-M. and Ayyub, H. (1990) A major positive regulatory region located far upstream of the human α-globin gene locus. *Genes Dev.*, **4**, 1588–1601.
23. Bitner-Glindzicz, M., de Kok, Y., Summers, D., Huber, I., Cremers, F.P.M., Ropers, H.-H., Reardon, W., Pembrey, M.E. and Malcolm, S. (1994) Close linkage of a gene for X linked deafness to three microsatellite repeats at Xq21 in radiologically normal and abnormal families. *J. Med. Genet.*, **31**, 916–921.
24. Reardon, W., Bellman, S., Phelps, P., Pembrey, M. and Luxon, L.M. (1993) Neuro-otological function in X-linked hearing loss: a multipedigree assessment and correlation with other clinical parameters. *Acta. Otolaryngol.*, **113**, 706–714.
25. Ayazi, S. (1981) Choroideremia, obesity and congenital deafness. *Am. J. Ophthalmol.*, 92, 63–69.
26. Nussbaum, R.L., Lesko, J.G., Lewis, R.A., Ledbetter, S.A. and Ledbetter, D.H. (1987) Isolation of anonymous DNA sequences from within a submicroscopic X chromosomal deletion in a patient with choroideremia, deafness, and mental retardation. *Proc. Natl Acad. Sci. USA*, **84**, 6521–6525.
27. Orita, M., Iwahana, H., Kanazawa, H., Hayashi, K. and Sekiya, T. (1989) Detection of polymorphisms of human DNA by gel electrophoresis as single-strand conformation polymorphisms. *Proc. Natl Acad. Sci. USA*, **86**, 2766–2770.
28. Suijkerbuijk, R.F., van de Veen, A.Y., van Echten, J., Buys, C.H.C.M., de Jong, B., Oosterhuis, J.W., Warburton, D.A., Cassiman, J.J., Schonk, D. and Geurts van Kessel, A. (1991) Demonstration of the genuine iso-12p character of the standard marker chromosome of testicular germ cell tumors and identification of further chromosome 12 aberrations by competitive in situ hybridization. *Am. J. Hum. Genet.*, **48**, 269–273.
29. Suijkerbuijk, R.F., Looijenga, L., de Jong, B., Oosterhuis, J.W., Cassiman, J.J. and Geurts van Kessel, A. (1992) Verification of isochromosome 12p and identification of other chromosome 12 aberrations in gonadal and extragonadal human germ cell tumors by bicolor double fluorescence in situ hybridization. *Cancer Genet. Cytogenet.*, **6**, 8–16.
30. Sinke, R.J., Suijkerbuijk, R.F., Herbergs, J., Janssen, H., Cassiman, J.J. and Geurts van Kessel, A. (1992) Generation of a panel of somatic cell hybrids containing fragments of human chromosome 12p by X-Ray irradiation and cell fusion. *Genomics*, **12**, 206–213.